

---

# Handwritten Text Recognition of Historical Manuscripts Using Transformer-Based Models

---

Erez Meoded

Department of Computer Science  
Mississippi State University  
em1748@msstate.edu

## Abstract

Historical manuscripts are invaluable for cultural and scholarly research, yet their digitization is hindered by limited transcriptions, language variation, and diverse handwriting styles. This paper investigates the use of `TrOCR`, a state-of-the-art transformer-based handwritten text recognizer, for 16<sup>th</sup>-century Latin manuscripts authored by Rudolf Gwalther. We evaluate the impact of targeted image preprocessing and a suite of data augmentation techniques, including four newly designed methods tailored to historical handwriting characteristics. We further explore ensemble learning to exploit the complementary strengths of augmentation-trained models. On the Gwalther dataset, our best single-model augmentation (Elastic) achieves a Character Error Rate (CER) of 1.86, while a top-5 voting ensemble reaches a CER of 1.60—representing a 50% relative improvement over the best reported `TrOCR_BASE` result and a 42% gain over the previous state of the art. These results demonstrate the effectiveness of domain-specific augmentations and ensemble strategies for advancing historical handwritten text recognition.

## 1 Introduction

Historical manuscripts are an essential source of original content, offering opportunities to connect and learn from the past. They are “regarded primarily if not exclusively as materials for research” [1]. While many archives of historical manuscripts exist, only a small portion are in digital, searchable formats. Handwritten Text Recognition (HTR) algorithms have been used to convert both modern and historical manuscripts from scanned images into machine-readable text. Early HTR systems employed imaging techniques such as Optical Character Recognition (OCR) scripting [2], feature-based classification and clustering [3], and feature word locating [4]. Later models integrated Artificial Intelligence (AI) approaches such as Hidden Markov Models (HMM) [5], Recurrent Neural Networks (RNN) [6], and CNN–RNN hybrid networks [7].

While modern AI models achieve high accuracy and efficiency for contemporary handwriting, historical manuscripts present three main challenges: (1) scarcity of transcriptions, as reliable labeled data is rare; (2) a language gap, since large language models are trained primarily on modern corpora; and (3) significant variation in handwriting styles between documents and time periods. These factors make training modern AI models for historical manuscripts difficult.

The introduction of the transformer architecture [8]—a parallel encoder–decoder framework using attention without RNN components—enabled significant performance gains in language and vision tasks. BERT [9] applied transformers to large-scale pretraining for transfer learning, and the Vision Transformer (ViT) [10] extended this approach to image inputs. This work

uses the transformer-based TrOCR model [11] and applies augmentations to recognize 16<sup>th</sup>-century Latin manuscripts. Augmentation and pretrained transformer-based models can help address the challenges outlined above. We evaluate the effectiveness of different augmentations on the performance of TrOCR for historical manuscripts.

### 1.1 Contributions

The contributions of this work are:

- An evaluation of the effectiveness of different augmentations on the performance of TrOCR.
- A demonstration that combining different augmentations via an ensemble of voters improves TrOCR performance.
- An application of TrOCR’s pluggable architecture to Latin text recognition.

## 2 Related Work

Research on Handwritten Text Recognition (HTR) has progressed from early feature-based systems to modern transformer-based architectures. Classical Optical Character Recognition (OCR) systems relied heavily on preprocessing, handcrafted feature extraction, and template matching [2, 3]. While effective for clean, machine-printed text, these methods struggled with the variability and degradation of historical manuscripts, which often exhibit irregular character shapes, inconsistent spacing, and complex backgrounds [1, 12, 13].

The introduction of attention mechanisms marked a significant shift in HTR, enabling models to focus selectively on relevant regions of the input. Early attention-based HTR systems typically combined Convolutional Neural Networks (CNNs) for feature extraction with sequential models such as Recurrent Neural Networks (RNNs), Long Short-Term Memory (LSTM) units, or Gated Recurrent Units (GRU) [14, 15]. These approaches captured temporal dependencies effectively but were constrained by sequential processing, limiting parallelization and efficiency.

Transformers [8] removed recurrence entirely, replacing it with multi-head self-attention and a fully parallel encoder–decoder architecture. This design improved modeling capacity over RNN-based systems but introduced quadratic complexity with respect to sequence length, which can be computationally expensive for high-dimensional image inputs.

To adapt transformers for vision tasks, the Vision Transformer (ViT) [10] treats an image as a sequence of fixed-size patches, enabling direct application of transformer layers without architectural changes. While ViT captures long-range dependencies well, its lack of inherent locality bias limits fine-grained structure recognition, which is important for handwriting. Subsequent hybrid models addressed this by incorporating convolutional layers before the transformer encoder [16].

TrOCR [11] is a fully transformer-based HTR system that combines a ViT encoder [10] with a RoBERTa [9] decoder. Huggingface’s implementation [17] replaces the decoder with XLM-RoBERTa [18], enabling multilingual recognition, including Latin script. TrOCR is pretrained in two stages—on large-scale printed text and then on synthetic handwritten text—and fine-tuned on various OCR tasks. Data augmentation plays a central role in improving robustness during fine-tuning. TrOCR is released in multiple sizes; prior work has primarily evaluated it on modern scripts, with less attention to historical Latin manuscripts.

Data augmentation is widely recognized as a key strategy for overcoming the scarcity of annotated historical data [11, 19–21]. Common augmentation techniques include rotation, translation, scaling, shearing [21], morphological operations such as erosion and dilation, Gaussian noise [22–25], blur, and random stretching. These augmentations simulate degradations such as curvature, ink fading, and scanning artifacts. However, relatively few studies have tailored augmentation specifically to the unique degradation patterns of 16<sup>th</sup>-century Latin manuscripts.

The primary evaluation metric in HTR is the Character Error Rate (CER) [26, 27], which measures normalized edit distance between predicted and reference text. CER remains the standard for quantifying recognition accuracy in both modern and historical contexts [1].

Historical manuscripts pose additional challenges beyond modern handwriting, including scarce transcriptions, layout distortions [12], variability in writing style, ink degradation, and cultural or linguistic variations [13]. While these sources hold significant historical value, limited work has explored transformer-based HTR methods combined with targeted augmentation strategies for this domain. Ensemble methods, although common in other vision tasks [28–32], have also seen limited application in historical HTR. Our work builds on these gaps by systematically evaluating augmentation strategies within TrOCR and integrating selective ensemble learning to improve recognition accuracy on historical Latin manuscripts.

### 3 Methodology

This section outlines the experimental methodology used to evaluate transformer-based handwritten text recognition (HTR) on 16<sup>th</sup>-century Latin manuscripts. The workflow proceeds from dataset preparation and preprocessing, through data augmentation and model training, to ensemble learning and evaluation procedures.

#### 3.1 Dataset and Preprocessing

Our experiments are based on 16<sup>th</sup>-century Latin manuscripts authored by Rudolf Gwalther (1519–1586), a pastor and head of the Reformed Church of Zurich during the Protestant Reformation [27]. High-resolution scans are publicly available through the *e-manuscripta* digital archive<sup>1</sup> [33].

Following [27], we use the processed dataset obtained by applying the AI-powered Handwritten Text Recognition service *Transkribus*<sup>2</sup> [34] to these digitized manuscripts. The recognition output, including PAGE-XML metadata with line-level coordinates and transcriptions, is publicly hosted on Zenodo<sup>3</sup> and referred to hereafter as the *Gwalther dataset*.

The dataset comprises 142 full-page manuscript images, each paired with a corresponding PAGE-XML annotation file. In total, there are 4,037 annotated text lines, each with a transcription and precise bounding box coordinates.

**Challenges.** Historical HTR presents specific difficulties [27]:

- Stains, faded ink, and paper degradation.
- Scribbled deletions or overwriting by original or later annotators.
- Upward curvature and skew of text lines.
- Non-uniform baseline alignment.
- Mixed handwriting styles, combining ornate calligraphy and simpler cursive.
- Background color variation and ink bleed-through.

These characteristics inform the augmentation strategies described in Sec. 3.2. Figure 1 illustrates typical examples.

**Preprocessing.** Since TrOCR accepts only single-line images, each full-page manuscript was segmented into individual line crops using PAGE-XML coordinates. Overlapping bounding boxes were manually corrected to ensure each crop contained exactly one complete line. To align with the visual characteristics of the IAM dataset [35] used in TrOCR’s pretraining, images were binarized to black text on a white background, normalized for background intensity, resized to the model’s expected input height, and padded as necessary to preserve aspect ratio.

---

<sup>1</sup><https://www.e-manuscripta.ch/zuz/doi/10.7891/e-manuscripta-26750>

<sup>2</sup><https://readcoop.eu/transkribus/>

<sup>3</sup><https://zenodo.org/record/4780947>

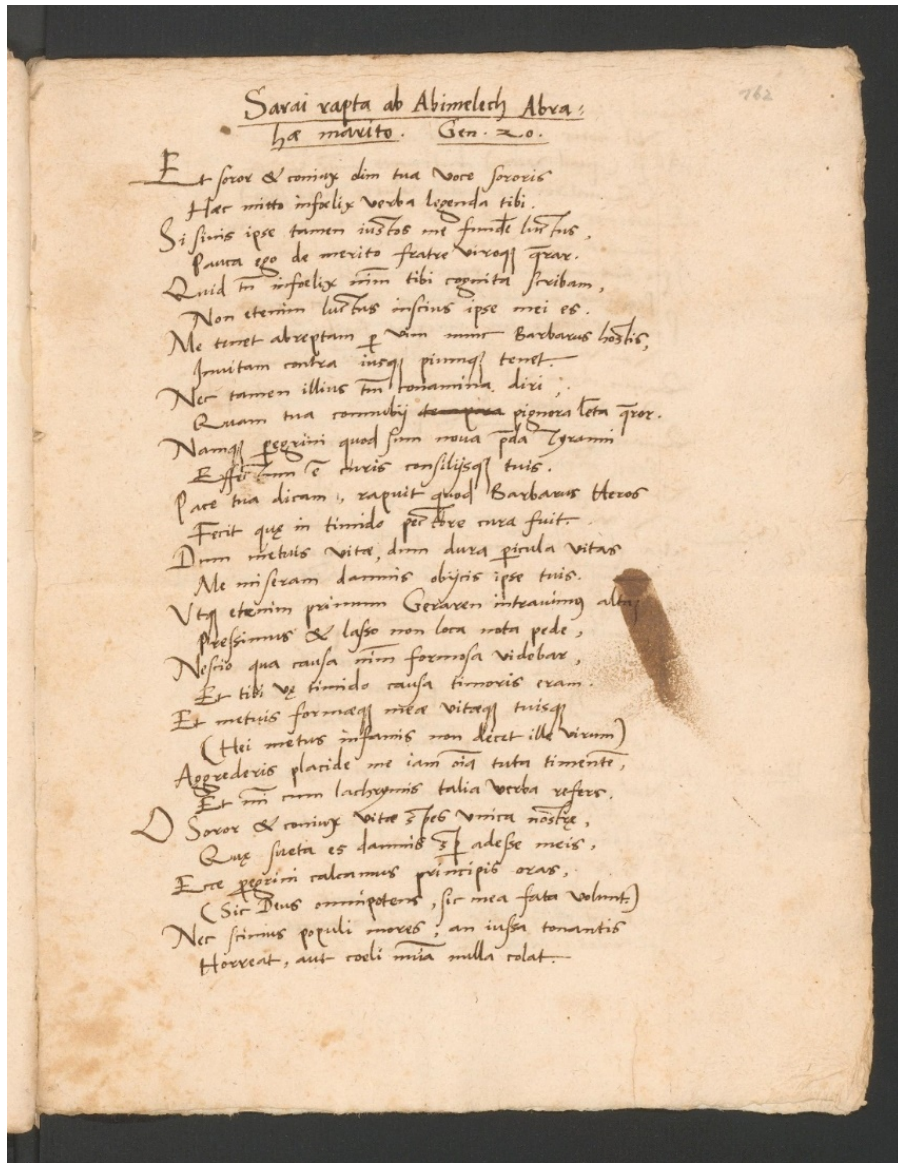


Figure 1: Sample manuscript page from the Gwalther dataset (file 1111637), exhibiting common historical HTR challenges.

Sarai rapta ab Abimelech Abra:  
ha manito. Gen. 20.  
Et soror & soror dim tua Noe sororis  
Hoc mitto infelix verba legenda tibi.  
Si soror ipse tuus in istis me fuisse latus.  
Paura ego de merito fratre viragi fratre.  
Quid tu infelix enim tibi cognita scribam.  
Non etenim luctus infans ipse mei es.  
Me tamen abreptam & non nunc Barbarus hostis,  
frontam contra iniqui pueri terret.  
Non tamen illius tan tonamilla dixi.  
Quam tua commubij deponit pueri tenui pro.  
Namque pugnari quod sum nua pila gramm  
Efficiunt & ducis consilios tuis.  
Pare tua dicam, rapuit quod Barbarus hostis  
Ferit que in timido pectore nra fuit.  
Dum metuus vita, dum dura puerula vita  
Me miseram dammis obijris ipse tuus.  
Vt etenim puerum Grecorum interauingulat  
Prestimis & lata non bona nata pede,  
Nescio qua causa minis formosa videbatur,  
Et tibi & timido causa timoris eram.  
Et metuus formosus mea vita tuisque  
(Hei metuus impars non decet illud virum)  
Agredieris placide me iam oia tuto timente,  
Et non non lachrymis talia verba refero.  
D Soror & soror nra & feliciter noster,  
Quae sueta es dammis & adeste meis,  
Ego pugnari valdeus pueris oras.  
(Si Deus omnipotens, sic mea fata voluntus)  
Non si nos populi mores; an iusta tonantis  
Horrent, aut coeli nra nulla rotat.

Figure 2: First three cropped and binarized lines from Figure 1 after preprocessing.

**Dataset Split.** Following [27], we split the dataset into 3,603 training lines and 433 validation lines using Scikit-Learn’s `train_test_split` API [36], ensuring reproducibility and comparability with prior work.

## 3.2 Data Augmentation

To mitigate overfitting and increase robustness, we applied data augmentation tailored to historical manuscript degradation patterns [11, 19, 21–25]. Each augmentation simulates specific real-world imperfections such as curvature, ink irregularities, and scanning artifacts.

### 3.2.1 Augmentation Methods

We evaluated ten augmentation techniques in addition to the baseline (no augmentation). Six were adapted from the original TrOCR handwritten text pipeline [11], with minor implementation fixes:

- a) Random Rotation — simulates text line curvature.
- b) Gaussian Blur — emulates optical or scanning blur.
- c) Dilation — thickens strokes, mimicking ink bleed.
- d) Erosion — thins strokes, simulating faded ink.
- e) Resize — alters resolution, representing scaling artifacts.
- f) Underline — adds synthetic underlines as seen in annotated manuscripts.

Four custom augmentations were introduced to better match the Gwalthmer dataset:

- g) Elastic Distortion [22] — mimics handwriting irregularities and ink flow variations.
- h) Random Affine — applies shearing and scaling to simulate layout distortion.
- i) Random Perspective — replicates camera-angle distortions in digitization.
- j) Re Resize — repeated resizing to introduce interpolation artifacts.

### 3.2.2 Application Strategy

For each augmentation method, a separate model was trained (ten augmented models plus one baseline). Augmentation was applied *on-the-fly* with probability  $p = 0.5$  per sample to balance diversity with data fidelity. No model combined multiple augmentation types, enabling direct comparison of individual effects. Evaluation of augmentation effectiveness is presented in Sec. 4.

## 3.3 Model Architecture and Training Setup

We used the Huggingface implementation [17] of TrOCR\_BASE [11], a transformer-based encoder–decoder model. The encoder is a Vision Transformer (DeiT [17]) with a Conv2d patch embedding layer, and the decoder is XLM-RoBERTa [18], enabling multilingual recognition.

**Pretraining.** TrOCR was pretrained in two stages [11]: (1) 684M lines from PDF text, and (2) 17.9M lines of synthetic handwritten text. Only Stage 1 weights are publicly available [37], which we use to initialize our models.

**Fine-tuning.** Each model (baseline and augmentation variants) was fine-tuned separately using hyperparameters from the original handwritten fine-tuning setup [35]:

- Optimizer: Adam [38] ( $\beta_1 = 0.9, \beta_2 = 0.999$ )
- Learning rate:  $3 \times 10^{-5}$
- Batch size: 16
- Loss: Cross-entropy with label smoothing = 0.1

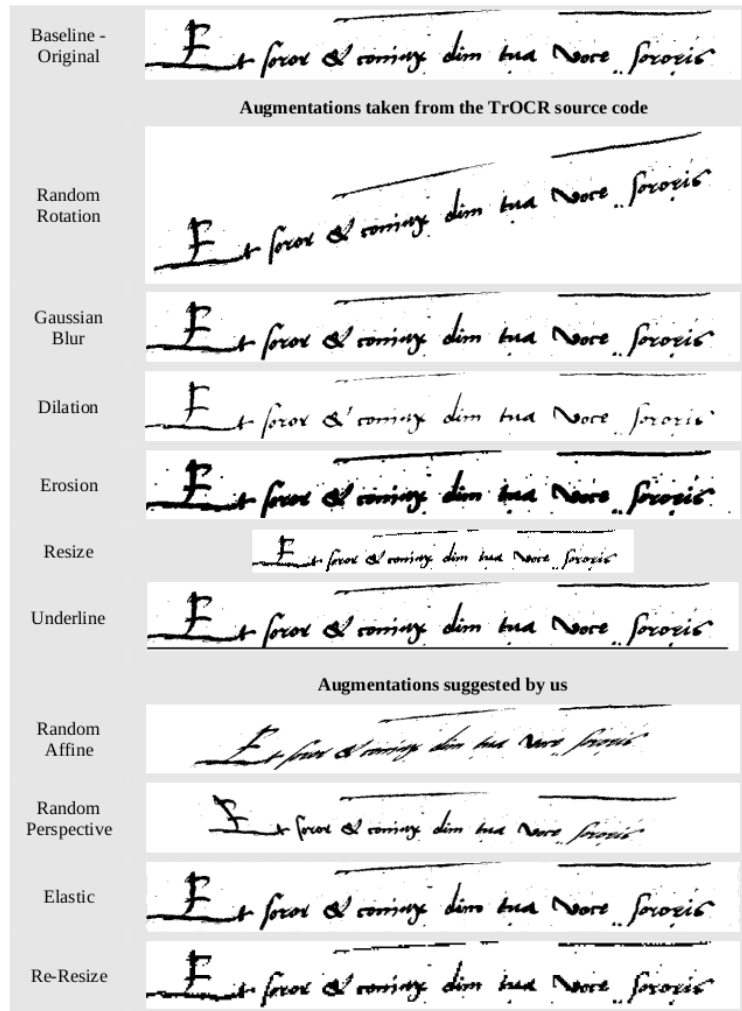


Figure 3: Baseline (no augmentation) and ten augmentation techniques evaluated in this work.

- Epochs: 20

Training was performed on Google Colab Pro+ with an NVIDIA A100 GPU (40 GB VRAM), requiring approximately one hour per model.

### 3.4 Ensemble Learning

Since individual augmentation strategies capture different aspects of handwriting variability, we employed ensemble learning to exploit complementary model strengths [28–32].

#### 3.4.1 Ensemble Configurations

Two sentence-level majority-voting strategies were tested:

**Ensemble A (Full Voting):** All eleven models (baseline + ten augmentations).

**Ensemble B (Top-5 Voting):** Five models with highest validation F1 scores: *Elastic Distortion*, *Random Rotation*, *Underline*, *Gaussian Blur*, and *Baseline*.

For each input line, each model generated its top-5 beam search hypotheses. All hypotheses were aggregated, and the sentence with the highest vote count was selected. Evaluation of ensemble performance is presented in Sec. 4.

#### 3.4.2 Character-Level Voting

We also tested character-level voting, selecting the most frequent character at each position. While it improved recognition of certain characters, it sometimes produced inconsistent outputs (e.g., mixed scripts within words) and was excluded from the final evaluation.

### 3.5 Evaluation and Analysis Tools

**Primary Metric.** The Character Error Rate (CER) [26, 27] is defined as:

$$\text{CER} = \frac{S + D + I}{N} \quad (1)$$

where  $S$  = substitutions,  $D$  = deletions,  $I$  = insertions, and  $N$  is the total number of characters in the reference transcription.

**Additional Metrics.** Precision, recall, and F1-score were computed at the character level to capture accuracy and completeness. We also monitored training and validation loss per epoch. Analysis of per-character F1 distributions and confusion patterns is provided in Sec. 4.

### Section Summary

This methodology integrates a carefully prepared historical manuscript dataset, targeted data augmentations, and ensemble learning to improve TrOCR-based HTR. Each component was designed to address specific degradation patterns and to enhance generalization, with effectiveness assessed in Sec. 4.

## 4 Results

This section presents evaluation outcomes for eleven models—one baseline without augmentation, six augmentation variants from the original TrOCR implementation, and four custom augmentations—on the 16<sup>th</sup>-century Gwalther manuscript dataset. We report Character Error Rate (CER) as the primary metric, supplemented by precision, recall, F1-score, qualitative examples, and ensemble learning results. All models were fine-tuned using identical hyperparameters on the TrOCR\_BASE architecture, with no additional tuning between variants.

	Baseline	CER Augmentations										Epochs
		Random Rotation	Gaussian Blur	Dilation	Erosion	Resize	Underline	Random Affine	Random Perspective	Elastic	Re Resize	
1	6.01	5.65	5.21	6.85	7.37	6.11	5.76	5.73	6.83	5.65	5.25	-1
2	4.19	4.02	4.12	5.12	4.71	4.35	4.28	4.32	4.89	4.26	4.34	-2
3	3.74	3.56	3.62	4.58	5.3	3.87	4.28	4.29	4.68	3.75	3.51	-3
4	3.27	3.23	2.91	4.76	3.6	3.75	3.43	3.42	3.69	3.13	3.24	-4
5	3.06	3.28	3.19	3.91	3.49	3.59	3.17	3.28	3.88	3.18	3.22	-5
6	3	2.89	3.07	3.71	3.45	3.21	2.94	5.32	3.28	3.18	3.16	-6
7	2.99	2.77	2.81	3.44	3.36	2.95	2.82	3	3.29	3.2	2.94	-7
8	2.63	2.79	2.64	3.42	3.49	3.08	2.61	2.86	3.13	2.8	2.95	-8
9	2.53	2.54	2.9	3.2	2.94	3.08	2.65	3.12	2.83	2.58	2.61	-9
10	2.49	2.42	2.44	3.15	2.87	2.75	2.51	2.56	2.79	2.54	2.83	-10
11	2.4	2.32	2.66	3.1	2.81	2.66	2.55	2.75	2.88	2.61	2.55	-11
12	2.41	2.26	2.65	3.12	2.72	2.73	2.37	2.58	2.72	2.42	2.62	-12
13	2.15	2.39	2.3	2.92	2.75	2.55	2.4	2.46	2.62	2.41	2.31	-13
14	2.19	2.32	2.2	2.61	2.66	2.54	2.19	2.49	2.58	2.33	2.17	-14
15	2.18	2	2.22	2.8	2.57	2.41	2.27	2.45	2.34	2.18	2.27	-15
16	2.14	2.09	2.11	2.81	2.6	2.49	2.23	2.1	2.47	1.9	2.09	-16
17	2.16	2.2	2.01	2.24	2.39	2.4	2.24	2.23	2.3	2.01	2.06	-17
18	1.98	1.98	2.03	2.3	2.42	2.31	2.06	2.24	2.27	1.9	2.1	-18
19	1.91	1.88	2	2.32	2.42	2.26	2.08	2.16	2.29	1.86	2.09	-19
20	1.93	1.86	2.04	2.31	2.33	2.31	2.03	2.13	2.27	1.86	2.09	-20
	Baseline	Random Rotation	Gaussian Blur	Dilation	Erosion	Resize	Underline	Random Affine	Random Perspective	Elastic	Re Resize	

Figure 4: CER scores per augmentation model over training epochs. The first column represents the baseline; the next six columns correspond to original TrOCR augmentations, and the final four to custom augmentations.

#### 4.1 CER Trends Across Training

Figure 4 illustrates CER progression over 20 epochs. Across most models, CER drops sharply in the first 15 epochs before stabilizing. Two augmentation strategies—*Random Rotation* (TrOCR original) and *Elastic* (custom)—consistently outperform the baseline throughout training. By epoch 20, both reach a CER of 1.86, an absolute improvement of 0.07 (3.6% relative) over the baseline’s 1.93.

Minimal geometric or photometric distortions (e.g., Random Rotation, Elastic) tend to converge faster and achieve lower CERs than high-distortion augmentations. In contrast, augmentations such as Dilation and Resize yield higher final CERs, suggesting excessive distortion can hinder model learning.

Table 1 summarizes final-epoch results, sorted by CER. The best-performing augmentations—Random Rotation and Elastic—are tied at 1.86, while the baseline ranks third at 1.93.

Table 1: Final-epoch (20) CER by augmentation type.

Epoch	Source	CER	Augmentation
20	TrOCR	1.86	Random Rotation
20	Ours	1.86	Elastic
20	Benchmark	1.93	Baseline
20	TrOCR	2.03	Underline
20	TrOCR	2.04	Gaussian Blur
20	Ours	2.09	Re Resize
20	Ours	2.13	Random Affine
20	Ours	2.27	Random Perspective
20	TrOCR	2.31	Dilation
20	TrOCR	2.31	Resize

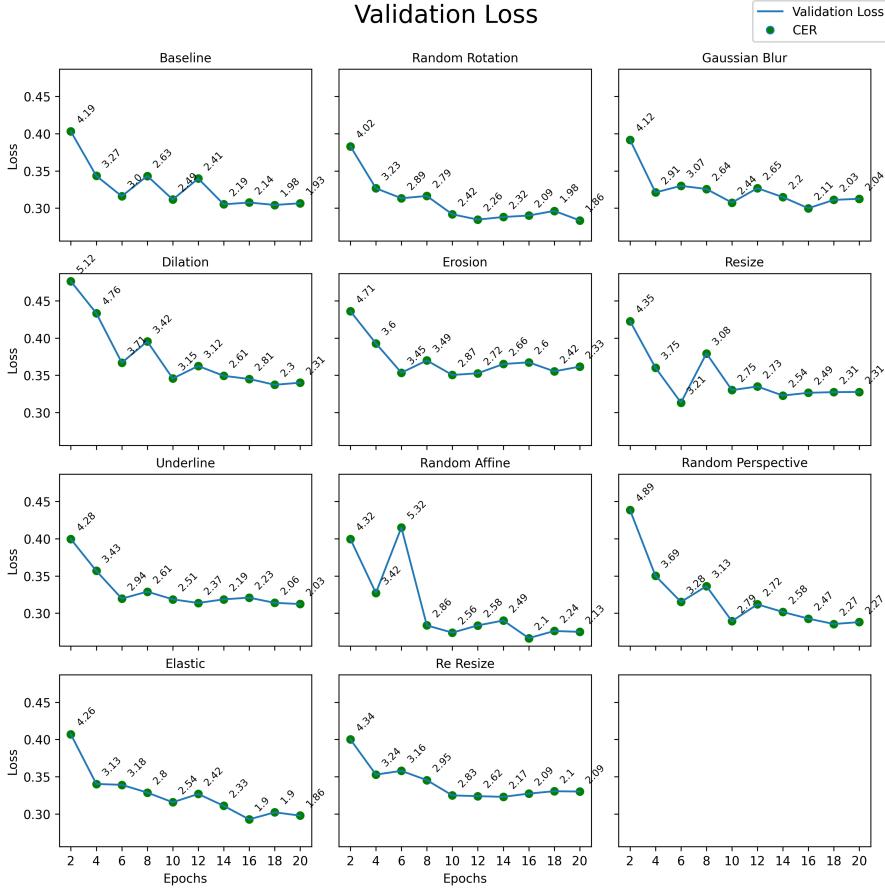


Figure 5: Validation loss at each even epoch, annotated with CER values.

## 4.2 Loss Convergence and CER Behavior

Validation loss trends in Figure 5 plateau after epoch 10, indicating convergence. Interestingly, CER may still improve slightly beyond this point, even when cross-entropy loss stabilizes or increases, highlighting that the two metrics capture different performance aspects.

Figures 6 and 7 confirm that Elastic and Random Rotation maintain their lead until convergence. The zoomed-in view of the final five epochs shows minimal fluctuation in CER, reflecting stable training dynamics in top models.

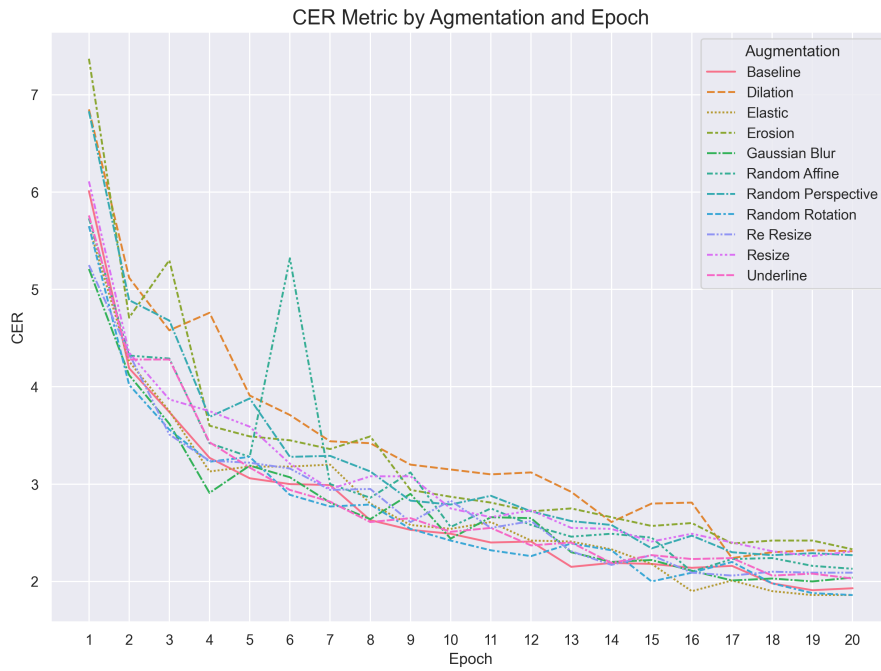


Figure 6: CER for each augmentation method over all 20 epochs.

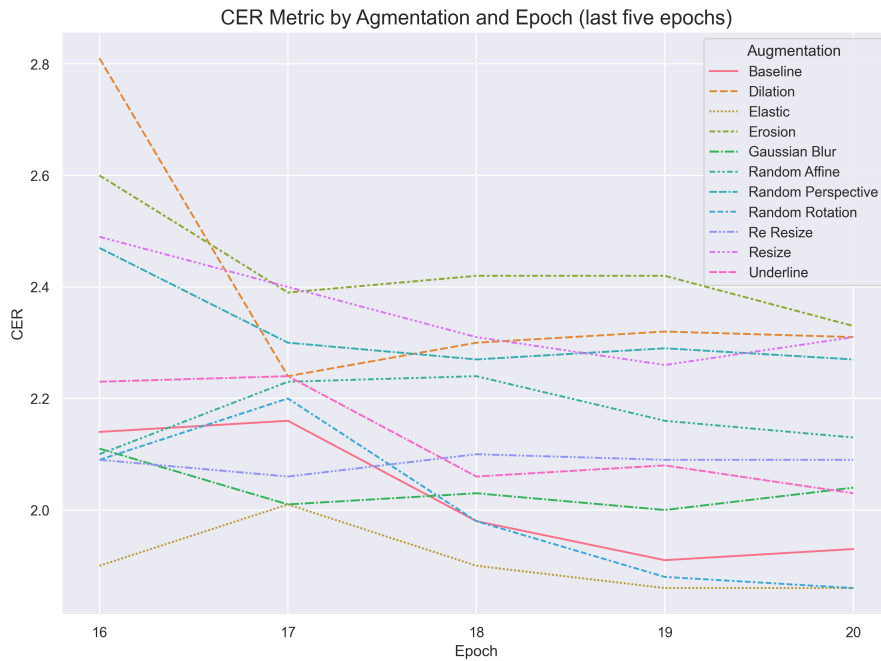


Figure 7: CER performance in the final five epochs, showing convergence and top-performing augmentations.

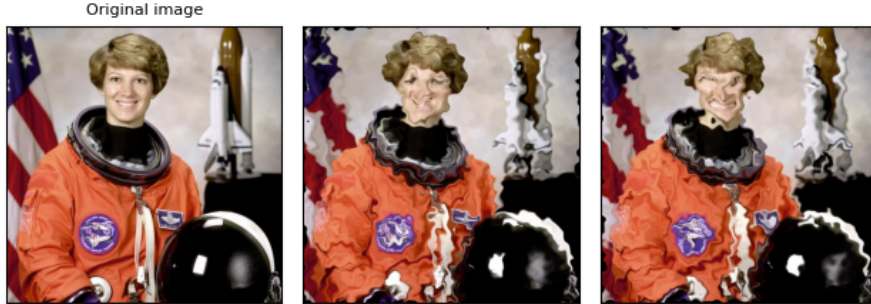


Figure 8: Example of Elastic Augmentation. Image source: [https://pytorch.org/vision/stable/auto\\_examples/plot\\_transforms.html#elastictransform](https://pytorch.org/vision/stable/auto_examples/plot_transforms.html#elastictransform)

	0.10	0.20	0.30	0.40	0.50	0.60	0.70	0.80	0.90	1.00
0.10	0.10	0.13	0.15	0.16	0.17	0.17	0.18	0.18	0.18	0.18
0.20	0.13	0.20	0.24	0.27	0.29	0.30	0.31	0.32	0.33	0.33
0.30	0.15	0.24	0.30	0.34	0.38	0.40	0.42	0.44	0.45	0.46
0.40	0.16	0.27	0.34	0.40	0.44	0.48	0.51	0.53	0.55	0.57
0.50	0.17	0.29	0.38	0.44	0.50	0.55	0.58	0.62	0.64	0.67
0.60	0.17	0.30	0.40	0.48	0.55	0.60	0.65	0.69	0.72	0.75
0.70	0.18	0.31	0.42	0.51	0.58	0.65	0.70	0.75	0.79	0.82
0.80	0.18	0.32	0.44	0.53	0.62	0.69	0.75	0.80	0.85	0.89
0.90	0.18	0.33	0.45	0.55	0.64	0.72	0.79	0.85	0.90	0.95
1.00	0.18	0.33	0.46	0.57	0.67	0.75	0.82	0.89	0.95	1.00

Figure 9: Relationship between F1, precision, and recall.

### 4.3 Elastic Augmentation Example

The custom *Elastic* augmentation, illustrated in Figure 8, simulates ink-flow irregularities and handwriting deformations. By introducing realistic imperfections, it likely enhances the model’s ability to generalize to authentic manuscript conditions, contributing to its competitive CER.

### 4.4 Character-Level Metrics

To complement CER, we computed precision, recall, and F1-score (Equations 2–4) to capture accuracy and completeness at the character level, revealing performance nuances not visible from CER alone.

$$\text{Precision} = \frac{\text{TP}}{\text{TP} + \text{FP}} \quad (2)$$

$$\text{Recall} = \frac{\text{TP}}{\text{TP} + \text{FN}} \quad (3)$$

$$F1 = \frac{2 \cdot \text{Precision} \cdot \text{Recall}}{\text{Precision} + \text{Recall}} \quad (4)$$

As shown in Figure 9, high F1 is achieved only when both precision and recall are high. Table 2 lists F1 scores for selected lowercase characters, revealing that *i* and *l* are consistently recognized well, while *m* and *n* remain more error-prone.

Table 2: F1 scores (scaled to 100) for selected lowercase characters across all models. Macro average is unweighted; weighted average is based on character frequency.

Character	Baseline	Rand. Rot.	Gauss. Blur	Dilation	Erosion	Resize	Underline	Rand. Affine	Rand. Persp.	Elastic	Re Resize
space	99.51	99.57	99.40	99.53	99.34	99.42	99.47	99.53	99.55	99.59	99.57
a	99.28	99.41	98.95	98.87	98.86	98.99	99.16	98.91	98.48	99.16	98.69
b	97.12	98.41	97.79	97.14	97.79	97.78	97.78	99.05	96.53	97.47	96.53
c	98.96	99.12	99.20	98.80	98.65	98.96	99.28	99.04	98.48	99.44	99.12
d	98.60	99.11	98.98	98.98	98.61	98.86	99.49	98.73	98.48	99.49	99.24
e	98.59	98.71	98.53	98.15	97.99	98.17	98.29	98.41	98.16	98.41	98.29
f	98.32	98.05	97.78	98.59	98.06	97.51	98.31	98.33	98.05	97.77	97.79
g	98.68	99.33	99.01	99.34	99.01	98.68	99.01	98.68	99.67	98.68	98.68
h	98.21	98.21	98.21	97.51	96.77	98.21	97.49	98.19	97.12	98.56	97.08
i	98.38	99.39	99.18	98.95	98.84	99.11	99.15	98.81	98.67	98.84	99.15
l	99.32	99.22	99.13	98.93	99.22	98.92	99.12	99.03	98.53	99.12	99.12
m	98.51	98.30	98.31	98.24	98.17	98.10	98.31	97.91	98.03	98.31	98.31
n	98.11	98.23	98.16	97.76	98.28	98.05	97.99	98.11	98.17	98.50	97.87
o	98.71	98.60	98.25	97.43	98.13	98.08	98.43	97.79	97.73	98.26	98.02
p	99.20	99.31	98.97	98.17	99.43	98.52	99.08	98.86	99.08	99.54	99.08
q	98.84	98.84	98.27	97.39	98.27	97.42	97.97	98.56	98.84	98.55	96.83
r	98.69	98.34	98.50	98.29	98.15	97.94	98.14	98.19	98.59	98.75	98.64
s	99.08	99.03	98.94	98.89	98.80	98.61	98.85	98.94	98.71	98.98	98.85
t	99.27	99.35	98.94	98.90	99.19	99.23	99.23	99.47	99.03	99.15	99.27
u	98.41	98.64	98.00	98.38	98.14	98.28	98.14	98.60	98.51	98.73	98.33
v	96.36	97.48	97.94	97.73	96.80	97.01	97.51	96.82	97.26	97.27	96.77
x	97.84	97.18	98.59	97.87	96.50	96.45	97.18	97.14	95.65	98.59	97.84
y	100.00	100.00	100.00	90.91	100.00	95.24	100.00	100.00	100.00	100.00	100.00
Accuracy	98.08	98.13	98.00	97.75	97.68	97.74	97.96	97.90	97.73	98.14	97.93
Macro Avg	80.79	83.36	78.34	80.61	81.52	84.22	78.08	83.66	82.39	82.87	82.49
Weighted Avg	98.26	98.26	98.09	97.90	97.61	97.90	98.03	97.90	98.25	98.03	98.03

Table 3: Predictions from various models for line 22 of file 1111690.

Model	Prediction
Baseline	Hei sed ferre sed hanc levig tu potes ipse moram.
Random Rotation	Heu ferre sed hanc levis tu potes ipse moram.
Gaussian Blur	He lectled ferre sed hanc levis tu potes ipse moram.
Dilation	He tibi servi sed hanc levius tu potes ipse moram.
Erosion	Hec tibi ded levior ferre sed hanc levis tu potes ipse moram.
Resize	Hei sed ferre sed hanc levique tu potes ipse moram.
Underline	He led ferne ferre sed hanc levis tu potes ipse moram.
Random Affine	Perre sed hanc levis tu potes ipse moram.
Random Perspective	Hei ferre sed hanc levius tu potes ipse moram.
Elastic	He ferre, ferre sed hanc levique tu potes ipse moram.
Re Resize	He deced ferre sed hanc levique tu potes ipse moram.
<b>Label (Ground Truth)</b>	<b>Ferre sed hanc levius tu potes ipse moram.</b>

Figure 10 shows the per-character distribution, while Figure 11 presents the aggregated confusion matrix. Frequent confusions occur between visually similar characters such as `m` and `n`.

#### 4.5 Ensemble Learning

Two sentence-level majority-voting ensembles were evaluated:

- **Full Voting** (all 11 models): CER = 1.66
- **Top-5 Voting** (Elastic, Random Rotation, Underline, Gaussian Blur, Baseline): CER = **1.60**

Given the average CER of individual models (2.11), both ensembles deliver substantial improvements, with Top-5 Voting achieving the largest gain—a 24% reduction relative to the mean single-model performance.

#### 4.6 Qualitative Examples

Three challenging transcription cases illustrate model behavior under adverse conditions:

##### 4.6.1 First Example

In this example, we examine line 22 from file 1111690 (Figure 12) and show the predictions from various augmentation models in Table 3. This line contains a deletion marked by an overline and an overflow from the top line, which introduces visual noise and complexity.

##### 4.6.2 Second Example

In this example, we examine line 15 from file 1111823 (Figure 13) and show how various augmentation models predict the text (Table 4). The first word in this line has excessive decorative strokes, and the second-to-last word includes a scribbled deletion, both of which challenge the recognition algorithms.

##### 4.6.3 Third Example

In this example, we examine line 0 from file 1111832 (Figure 14) and compare how various augmentation models perform in recognizing the line (Table 5). This line suffers from background noise—likely due to its position near the page edge and signs of aging—and is visually blurred, making it harder to recognize.

#### 4.7 Comparison to Prior Work

Our best ensemble achieves a CER of **1.60** on the Gwalther dataset, outperforming the prior best TrOCR<sub>BASE</sub> result (3.18) from [27] by 50%, and surpassing the previous state-of-the-art

Characters	F1 Augmentations												-a
	Baseline	Random Rotation	Gaussian Blur	Dilation	Erosion	Resize	Underline	Random Affine	Random Perspective	Elastic	Re Resize		
a	99.28	99.2	98.95	98.87	98.86	98.99	99.16	98.91	98.48	99.16	98.69	-a	
b	97.12	98.41	97.79	97.14	97.79	97.78	97.78	99.05	96.53	97.47	96.53	-b	
c	98.96	99.12	99.2	98.8	98.65	98.96	99.28	99.04	98.48	99.44	99.12	-c	
d	98.6	99.11	98.98	98.98	98.61	98.86	99.49	98.73	98.48	99.49	99.24	-d	
e	98.59	98.71	98.53	98.15	97.99	98.17	98.29	98.41	98.16	98.41	98.29	-e	
f	98.32	98.05	97.78	98.59	98.06	97.51	98.31	98.33	98.05	97.77	97.79	-f	
g	98.68	99.33	99.01	99.34	99.01	98.68	98.68	99.01	98.68	99.67	98.68	-g	
h	98.21	98.21	98.21	97.51	96.77	98.21	97.49	98.19	97.12	98.56	97.08	-h	
i	98.98	99.39	99.18	98.95	98.84	99.11	99.15	98.81	98.67	98.84	99.15	-i	
l	99.32	99.22	99.13	98.93	99.22	98.92	99.12	99.03	98.53	99.12	99.12	-l	
m	98.51	98.3	98.31	98.24	98.17	98.1	98.31	97.91	98.03	98.31	98.31	-m	
n	98.11	98.23	98.16	97.76	98.28	98.05	97.99	98.11	98.17	98.5	97.87	-n	
o	98.71	98.6	98.25	97.43	98.13	98.08	98.43	97.79	97.73	98.26	98.02	-o	
p	99.2	99.31	98.97	98.17	99.43	98.52	99.08	98.86	99.08	99.54	99.08	-p	
q	98.84	98.84	98.27	97.39	98.27	97.42	97.97	98.56	98.84	98.55	96.83	-q	
r	98.69	98.34	98.5	98.29	98.15	97.94	98.14	98.19	98.59	98.75	98.64	-r	
s	99.08	99.03	98.94	98.89	98.8	98.61	98.85	98.94	98.71	98.98	98.85	-s	
t	99.27	99.35	98.94	98.9	99.19	99.23	99.23	99.47	99.03	99.15	99.27	-t	
u	98.41	98.51	98.64	98	98.38	98.14	98.28	98.6	98.51	98.73	98.33	-u	
v	96.36	97.48	97.94	97.73	96.8	97.01	97.51	96.82	97.26	97.27	96.77	-v	
x	97.84	97.18	98.59	97.87	96.5	96.45	97.18	97.14	95.65	98.59	97.84	-x	
	Baseline	Random Rotation	Gaussian Blur	Dilation	Erosion	Resize	Underline	Random Affine	Random Perspective	Elastic	Re Resize		

Figure 10: F1 score distribution across lowercase characters.

Table 4: Predictions from various models for line 15 of file 1111823.

Model	Prediction
Baseline	Et nimiis mersus coecus vernas aquis.
Random Rotation	Et nimiis mersus coecus somnas aquis.
Gaussian Blur	Et nimiis mersus coecus formas aquis.
Dilation	Et nimiis mersus coecus Iothas aquis.
Erosion	Et nimiis mersus coecus formas aquis.
Resize	Et nimiis mersus coecus fortnas aquis.
Underline	Et nimiis mersus coecus vernas aquis.
Random Affine	Et nimiis mersus coecus poenas aquis.
Random Perspective	Et nimiis mersus coecus poenas aquis.
Elastic	Et nimis mersus coecus Iottinas aquis.
Re Resize	Est nimiis mersus coecus formas aquis.
<b>Label (Ground Truth)</b>	<b>Est nimiis mersus coecus Ionas aquis.</b>

		Confusion Matrix																					
		Predictions																					
True Labels	a	b	c	d	e	f	g	h	i	l	m	n	o	p	q	r	s	t	u	v	x	y	
	a	0	0	0.1	0.3	2	0	0	0.2	0.5	0.1	0.1	0.4	1.4	0	0.2	0.8	0.6	0	1.5	0	0	
	b	0.1	0	0.2	0.1	0.1	0	0	0.1	0	0.2	0.1	0.3	0	0	0	0.1	0	0.1	0.4	0	0	
	c	0.7	0.1	0	0	0.6	0	0	0.1	0.8	0	0	0.1	0	0.1	0.1	0.1	0.4	1.5	0.1	0.1	0	
	d	0	0.1	0	0	0	0	0	0	0.1	0	0	0	0	0.1	0	0.1	0.2	0.2	0	0.1	0	
	e	2.8	0.1	1.3	0	0	0	0	1.8	0	0	0.2	5.3	0.4	0.3	0.7	0.5	0.4	2.1	0	0	0	
	f	0	0	0	0	0	0	0.3	0	0.1	0	0.2	0	0	0.1	0	0.1	0.5	0.2	0	0.1	0	
	g	0	0.1	0.4	0	0	0	0	0	0	0	0	0	0	0.5	0	0	0.1	0	0	0	0	
	h	0	0.4	0	0.1	0	0.2	0	0	0.1	0.2	0.1	0.1	0	0	0.1	0.5	0.1	0	0	0	0	
	i	0.4	0.3	0.1	0.1	1.5	0	0	0	0	0.9	0.2	0.8	0	0.1	0.9	0.3	0.2	2.2	0	0	0	
	l	0.5	0.3	0	1	0.1	0.5	0	0.1	0	0	0.3	0	0	0	0.4	0.2	2	0	0.1	0	0	
	m	0.7	0	0.1	0.2	0.1	0	0	0	0.1	0	0	5.5	0.3	0	0.2	0.7	0.3	0.2	0.1	0	0.5	
	n	1	0.1	0.4	0.2	0.2	0	0	0.4	0.5	0	7.7	0	0.4	0.1	0	1.5	0.9	0.7	0.7	0.5	0	
	o	1.8	0.1	0	0.1	4.4	0	0	0	1.9	0.1	0.2	0.1	0	0.2	0	0.5	0.3	0.2	1.3	0	0.1	
	p	0	0.1	0	0	0.1	0.1	0	0	0.4	0	0	0	0	0	0.4	0	0	0.1	0.2	0.1	0	
	q	0	0	0	0	0	0	0	0	0	0	0	0	0	0.9	0	0	0	0	0	0	0	
	r	0.2	0.1	0.2	0	1	0	0	0	0.1	0.1	0.3	0.5	0.5	0.3	0.4	0	0.5	0.6	0.6	0.2	0.2	0
	s	0.8	0.1	0	0	1.2	1.4	0.4	0	0.2	0	0.2	0.3	0.9	0.7	0.1	0.3	0	0.2	1	0	0.5	0
	t	0	0.2	0.4	0.5	0.4	0	0.1	0.1	0.3	0.3	0.4	0	0.4	0	0	0.5	0.8	0	0.1	0	0	
	u	1	0.5	0.1	0	1.5	0	0	0.1	1.4	0	0	0.6	0.5	0	0.3	1.1	0.1	1.1	0	2.1	0	0
	v	0	0	0.1	0	0	0	0	0	0.1	0	0.1	1	0	0	1	0.8	0.1	0	2.1	0	1	0
	x	0	0	0.1	0	0	0.1	0	0	0	0	0	0.1	0.3	0	0	0	0.2	0	0.5	0	0	
	y	0	0	0	0	0	0	0	0	0	0	0	0	0	0	0	0	0	0	0	0	0	

Figure 11: Aggregated confusion matrix over all models.

~~He reis fand keine Fische und kann keinen in portos ipsi mora.~~

Figure 12: Line 22 from file 1111690

~~Est minus meritus vocans Iohannas aquas.~~

Figure 13: Line 15 from file 1111823

~~De nos feda miti causa Libido fruct.~~

Figure 14: Line 0 from file 1111832

Table 5: Predictions from various models for line 0 of file 1111832.

Model	Prediction
Baseline	Quorum foedera mihi causa libido fuit.
Random Rotation	Quorum foedera mihi causa libido fuit.
Gaussian Blur	Quorum foedera mihi causa libido fuit.
Dilation	Quorum fada mihi causa libido fuit.
Erosion	Quorum foeda mihi causa libido fuit.
Resize	Quorum foedera mihi causa libido fuit.
Underline	Quorum foedera mihi causa libido fuit.
Random Affine	Quorum foedera mihi causa libido fuit.
Random Perspective	Quorum foedera mihi causa libido fuit.
Elastic	Quorum foeder mihi causa libido fuit.
Re Resize	Quorum foeda midi causa libido fuit.
<b>Label (Ground Truth)</b>	<b>Quorum foeda mihi causa Libido fuit.</b>

HTR+ (2.74) by 42%. We attribute this improvement to careful line-level preprocessing, which aligns inputs with TrOCR’s pre-training format and enhances recognition accuracy.

## 5 Discussion

Our experiments demonstrate that targeted data augmentation can substantially improve transformer-based HTR performance on historical manuscripts. Among the techniques evaluated, *Elastic Distortion* delivered the largest single-model gain, indicating that local geometric perturbations are particularly effective in modeling the natural warping and curvature present in handwritten text on aged paper. This observation is consistent with prior findings in historical document processing [1, 12].

Preprocessing proved essential for achieving stable and accurate recognition. Steps such as grayscale conversion, deskewing, and consistent image height normalization reduced variability across inputs, thereby improving convergence and generalization. Furthermore, adopting a writer-independent dataset split ensured that performance gains reflect genuine robustness to unseen handwriting styles, rather than overfitting to specific scribes.

Ensemble learning provided a further boost, reducing CER from 1.86 for the best single model to 1.60 for the Top-5 Voting ensemble (Sec. 4). The complementary strengths of differently augmented models allowed the ensemble to correct systematic errors—particularly in cases involving ligatures, uncommon letterforms, and complex stroke connections.

Despite these gains, certain challenges remain. Historical Latin abbreviations often require contextual expansion rather than direct transcription, a task beyond the capabilities of our purely visual model. Additionally, recognition of diacritics was inconsistent, especially under severe fading or background noise. Addressing these limitations may require integrating external linguistic resources, specialized abbreviation expansion rules, or post-processing correction modules informed by historical orthography.

**Implications for Historical HTR.** The results highlight that transformer-based HTR systems can benefit significantly from augmentations tailored to the specific degradation patterns of historical sources, and that selective ensembling can yield gains beyond any single model. These findings suggest that, for low-resource historical scripts, model diversity through augmentation is as important as raw model capacity. By aligning preprocessing with pretraining domain characteristics and exploiting complementary inductive biases from different augmentations, researchers can push recognition accuracy closer to practical usability for large-scale transcription projects, even when annotated data are scarce.

## 6 Conclusion

We presented a systematic evaluation of augmentation techniques and ensemble learning for TrOCR-based recognition of 16<sup>th</sup>-century Latin manuscripts. Our experiments show that

targeted, domain-specific augmentations can reduce the Character Error Rate by nearly half compared to a non-augmented baseline, and that selective ensembles of augmentation-trained models provide additional gains, achieving new state-of-the-art performance on the Gwalther dataset.

Future work will explore:

- Combining multiple augmentations during training to assess potential synergies and further enhance generalization.
- Incorporating language models specialized for historical Latin to improve abbreviation expansion and rare word recognition.
- Extending the evaluation to additional historical handwriting corpora to assess cross-domain generalizability.

The proposed augmentation and ensemble strategies are straightforward to implement and applicable to other low-resource HTR contexts. By improving recognition accuracy in challenging historical settings, these methods contribute to the broader effort of preserving and digitizing cultural heritage at scale.

## Code Availability

The source code for the experiments in this paper is publicly available at <https://github.com/erez-meoded/TrOCR-HTR>.

## References

- [1] L. J. Cappon. Historical manuscripts as archives: some definitions and their application. *The American Archivist*, 19(2):101–110, 1956. doi: 10.17723/aarc.19.2.4402r63w3t257gv8.
- [2] J. I. Makhoul, R. Schwartz, C. LaPre, and I. Bazzi. A script-independent methodology for optical character recognition. *Pattern Recognition*, 31(9):1285–1294, 1998.
- [3] L. Wolf, L. Potikha, N. Dershowitz, R. Shweka, and Y. Choueka. Computerized paleography: tools for historical manuscripts. In *2011 18th IEEE International Conference on Image Processing (ICIP)*, pages 3545–3548, Brussels, Belgium, September 2011. IEEE. doi: 10.1109/ICIP.2011.6116481.
- [4] T. M. Rath and R. Manmatha. Features for word spotting in historical manuscripts. In *Proceedings of the Seventh International Conference on Document Analysis and Recognition (ICDAR)*, pages 218–222, Edinburgh, UK, 2003. IEEE Computer Society. doi: 10.1109/ICDAR.2003.1227662.
- [5] J. A. Rodríguez-Serrano and F. Perronnin. A model-based sequence similarity with application to handwritten word spotting. *IEEE Transactions on Pattern Analysis and Machine Intelligence*, 34(11):2108–2120, November 2012. doi: 10.1109/TPAMI.2012.25.
- [6] V. Frinken, A. Fischer, R. Manmatha, and H. Bunke. A novel word spotting method based on recurrent neural networks. *IEEE Transactions on Pattern Analysis and Machine Intelligence*, 34(2):211–224, February 2012. doi: 10.1109/TPAMI.2011.113.
- [7] K. Dutta, P. Krishnan, M. Mathew, and C. V. Jawahar. Improving cnn-rnn hybrid networks for handwriting recognition. In *2018 16th International Conference on Frontiers in Handwriting Recognition (ICFHR)*, pages 80–85, Niagara Falls, USA, August 2018. IEEE. doi: 10.1109/ICFHR-2018.2018.00023.
- [8] A. Vaswani, N. Shazeer, N. Parmar, J. Uszkoreit, L. Jones, A. N. Gomez, Ł. Kaiser, and I. Polosukhin. Attention is all you need. *arXiv preprint arXiv:1706.03762*, June 2017. doi: 10.48550/arXiv.1706.03762.

[9] J. Devlin, M.-W. Chang, K. Lee, and K. Toutanova. Bert: pre-training of deep bidirectional transformers for language understanding. *arXiv preprint arXiv:1810.04805*, May 2019. doi: 10.48550/arXiv.1810.04805.

[10] A. Dosovitskiy, L. Beyer, A. Kolesnikov, D. Weissenborn, X. Zhai, T. Unterthiner, M. Dehghani, M. Minderer, G. Heigold, S. Gelly, J. Uszkoreit, and N. Houlsby. An image is worth  $16 \times 16$  words: transformers for image recognition at scale. *arXiv preprint arXiv:2010.11929*, June 2021. doi: 10.48550/arXiv.2010.11929.

[11] M. Li, T. Lv, J. Chen, L. Cui, Y. Lu, D. A. F. Florêncio, C. Zhang, Z. Li, and F. Wei. Trocr: transformer-based optical character recognition with pre-trained models. *arXiv preprint arXiv:2109.10282*, September 2021. doi: 10.48550/arXiv.2109.10282.

[12] E. Chammas, C. Mokbel, and L. Likforman-Sulem. Handwriting recognition of historical documents with few labeled data. In *2018 13th IAPR Int. Workshop on Document Analysis Systems (DAS)*, pages 43–48. IEEE, April 2018. doi: 10.1109/DAS.2018.15.

[13] E. S. M. Penn. *Exploring archival value: an axiological approach*. Phd thesis, University College London, 2014.

[14] D. Bahdanau, K. Cho, and Y. Bengio. Neural machine translation by jointly learning to align and translate. *arXiv preprint arXiv:1409.0473*, 2014. doi: 10.48550/arXiv.1409.0473.

[15] K. Cho, B. van Merriënboer, D. Bahdanau, and Y. Bengio. On the properties of neural machine translation: encoder–decoder approaches. In *Proc. of SSST-8, Eighth Workshop on Syntax, Semantics and Structure in Statistical Translation*, pages 103–111, Doha, Qatar, 2014. Association for Computational Linguistics. doi: 10.3115/v1/W14-4012.

[16] Y. Li, K. Li, J. Cao, R. Timofte, and L. Van Gool. Localvit: bringing locality to vision transformers. *arXiv preprint arXiv:2104.05707*, April 2021. URL <http://arxiv.org/abs/2104.05707>. Accessed: Jul. 26, 2023.

[17] T. Wolf, L. Debut, V. Sanh, J. Chaumond, C. Delangue, A. Moi, P. Cistac, T. Rault, R. Louf, M. Funtowicz, J. Davison, S. Shleifer, P. von Platen, C. Ma, Y. Jernite, J. Plu, C. Xu, T. Le Scao, S. Gugger, M. Drame, Q. Lhoest, and A. M. Rush. Huggingface’s transformers: state-of-the-art natural language processing. *arXiv preprint arXiv:1910.03771*, July 2020. doi: 10.48550/arXiv.1910.03771.

[18] A. Conneau, K. Khandelwal, N. Goyal, V. Chaudhary, G. Wenzek, F. Guzmán, É. Grave, M. Ott, L. Zettlemoyer, and V. Stoyanov. Unsupervised cross-lingual representation learning at scale. *arXiv preprint arXiv:1911.02116*, April 2020. doi: 10.48550/arXiv.1911.02116.

[19] J. Han, T. He, Y. Lin, Z. Lai, J. Lin, C. Gan, and S. Han. You only cut once: boosting data augmentation with a single cut. In *Proc. of the 39th Int. Conf. on Machine Learning*, pages 8196–8212. PMLR, June 2022. URL <https://proceedings.mlr.press/v162/han22a.html>. Accessed: Jul. 26, 2023.

[20] A. Bansal, R. Sharma, and M. Kathuria. A systematic review on data scarcity problem in deep learning: solution and applications. *ACM Computing Surveys*, 54(10s):208:1–208:29, September 2022. doi: 10.1145/3502287.

[21] S. Minz, R. Kanodia, T. Yadav, and N. Jayanthi. Enhancing accuracy in handwritten text recognition with convolutional recurrent neural network and data augmentation techniques. In *Proc. of the 2023 Third Int. Conf. on Secure Cyber Computing and Communication (ICSCCC)*, pages 803–808. IEEE, May 2023. doi: 10.1109/ICSCCC58608.2023.10176601.

[22] J. Puigcerver. Are multidimensional recurrent layers really necessary for handwritten text recognition? In *2017 14th IAPR Int. Conf. on Document Analysis and Recognition (ICDAR)*, pages 67–72, Kyoto, Japan, November 2017. IEEE. doi: 10.1109/ICDAR.2017.20.

[23] A. F. de Souza Neto, B. L. D. Bezerra, A. H. Toselli, and E. B. Lima. A robust handwritten recognition system for learning on different data restriction scenarios. *Pattern Recognition Letters*, 159:232–238, July 2022. doi: 10.1016/j.patrec.2022.04.009.

[24] T. Wilkinson and A. Brun. Semantic and verbatim word spotting using deep neural networks. In *15th Int. Conf. on Frontiers in Handwriting Recognition (ICFHR)*, pages 307–312, Shenzhen, China, 2016. IEEE Computer Society. doi: 10.1109/ICFHR.2016.0065.

[25] G. Retsinas, G. Sfikas, B. Gatos, and C. Nikou. Best practices for a handwritten text recognition system. In S. Uchida, E. Barney, and V. Eglin, editors, *Document Analysis Systems*, Lecture Notes in Computer Science, pages 247–259. Springer International Publishing, Cham, Switzerland, 2022. doi: 10.1007/978-3-031-06555-2\_17.

[26] J. A. Sánchez, V. Romero, A. H. Toselli, M. Villegas, and E. Vidal. A set of benchmarks for handwritten text recognition on historical documents. *Pattern Recognition*, 94: 122–134, October 2019. doi: 10.1016/j.patcog.2019.05.025.

[27] P. B. Ströbel, S. Clematide, M. Volk, and T. Hodel. Transformer-based htr for historical documents. *arXiv preprint arXiv:2203.11008*, March 2022. URL <http://arxiv.org/abs/2203.11008>. Accessed: Jul. 20, 2023.

[28] L. I. Kuncheva and C. J. Whitaker. Measures of diversity in classifier ensembles and their relationship with the ensemble accuracy. *Machine Learning*, 51(2):181–207, May 2003. doi: 10.1023/A:1022859003006.

[29] D. W. Opitz and R. Maclin. Popular ensemble methods: an empirical study. *Journal of Artificial Intelligence Research*, 11:169–198, August 1999. doi: 10.1613/jair.614.

[30] R. Polikar. Ensemble based systems in decision making. *IEEE Circuits and Systems Magazine*, 6(3):21–45, 2006. doi: 10.1109/MCAS.2006.1688199.

[31] L. Rokach. Ensemble-based classifiers. *Artificial Intelligence Review*, 33(1):1–39, February 2010. doi: 10.1007/s10462-009-9124-7.

[32] D. I. Mienye and Y. Sun. A survey of ensemble learning: concepts, algorithms, applications, and prospects. *IEEE Access*, 10:99129–99149, 2022. doi: 10.1109/ACCESS.2022.3207287.

[33] P. Stotz and P. Ströbel. bullinger-digital/gwalthther-handwriting-ground-truth: Initial release. Zenodo, May 2021.

[34] L. Seaward and M. Kallio. Transkribus: handwritten text recognition technology for historical documents. In *Digital Humanities 2017 (DH2017)*, 2017.

[35] H. Li, P. Chaudhari, H. Yang, M. Lam, A. Ravichandran, R. Bhotika, and S. Soatto. Rethinking the hyperparameters for fine-tuning. *arXiv preprint arXiv:2002.11770*, February 2020. doi: 10.48550/arXiv.2002.11770.

[36] F. Pedregosa, G. Varoquaux, A. Gramfort, V. Michel, B. Thirion, O. Grisel, M. Blondel, P. Prettenhofer, R. Weiss, V. Dubourg, J. VanderPlas, A. Passos, D. Cournapeau, M. Brucher, M. Perrot, and É. Duchesnay. Scikit-learn: machine learning in python. *Journal of Machine Learning Research*, 12:2825–2830, 2011.

[37] Y. Liu, M. Ott, N. Goyal, J. Du, M. Joshi, D. Chen, O. Levy, M. Lewis, L. Zettlemoyer, and V. Stoyanov. Roberta: a robustly optimized bert pretraining approach. *arXiv preprint arXiv:1907.11692*, July 2019. doi: 10.48550/arXiv.1907.11692.

[38] M. Subramanian, K. Shanmugavadiel, and P. S. Nandhini. On fine-tuning deep learning models using transfer learning and hyper-parameter optimization for disease identification in maize leaves. *Neural Computing and Applications*, 34(16):13951–13968, August 2022. doi: 10.1007/s00521-022-07246-w.